Lecture 30. Waveguide coupling and Integrated Electro-Optic Modulators

Coupling between two modes.

Consider waveguide with multiple modes propagating. We select just two modes as in Fig. 30.1 , so the fields are

$$\begin{aligned} \boldsymbol{E} &= \sum_{m=1}^{2} \tfrac{1}{2} A_m(z) e^{j(\beta_m z-\omega t)} \boldsymbol{e}_m(x,y) + c.c. \\ \boldsymbol{H} &= \sum_{m=1}^{2} \tfrac{1}{2} A_m(z) e^{j(\beta_m z-\omega t)} \boldsymbol{h}_m(x,y) + c.c. \end{aligned} \tag{30.1}$$

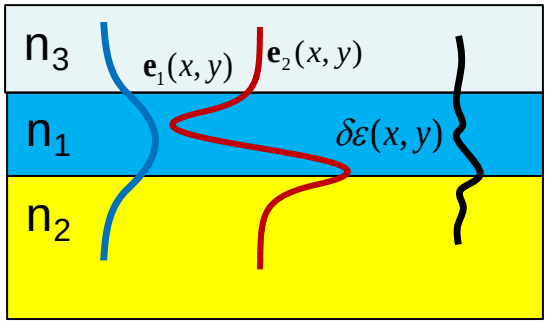

Figure 30.1 Waveguide mode coupling

Substitute it into the Maxwell's equations

$$\begin{aligned} \nabla \times \boldsymbol{E} &= j\omega\mu_0 \boldsymbol{H} \\ \nabla \times \mathbf{H} &= -j\omega\varepsilon_0\varepsilon_r \boldsymbol{E} \end{aligned} \tag{30.2}$$

and obtain

$$\begin{aligned} \sum_{m=1}^{2} \left(A_m \nabla_\perp \times \boldsymbol{e}_m + jA_m\beta_m \hat{\mathbf{z}} \times \boldsymbol{e}_m + \frac{dA_m}{dz} \hat{\mathbf{z}} \times \boldsymbol{e}_m \right) e^{j\beta_m z} &= j \sum_{m=1}^{2} A_m \omega\mu \boldsymbol{h}_m e^{j\beta_m z} \\ \sum_{m=1}^{2} \left(A_m \nabla_\perp \times \boldsymbol{h}_m + jA_m\beta_m \hat{\mathbf{z}} \times \boldsymbol{h}_m + \frac{dA}{dz} \hat{\mathbf{z}} \times \boldsymbol{h}_m \right) e^{j\beta_m z} &= -j \sum_{m=1}^{2} A_m \omega\varepsilon_0\varepsilon_r \boldsymbol{e}_m e^{j\beta_m z} \end{aligned} \tag{30.3}$$

Re-arrange the terms

$$\begin{aligned} \sum_{m=1}^{2} A_m \left(-\nabla_\perp \times \boldsymbol{e}_m + j\omega\mu \boldsymbol{h}_m \right) e^{j\beta_m z} &= \sum_{m=1}^{2} \left(jA_m\beta_m \hat{\mathbf{z}} \times \boldsymbol{e}_m + \frac{dA_m}{dz} \hat{\mathbf{z}} \times \boldsymbol{e}_m \right) e^{j\beta_m z} \\ \sum_{m=1}^{2} A_m \left(-\nabla_\perp \times \boldsymbol{h}_m - j\omega\varepsilon_0\varepsilon_r \boldsymbol{e}_m \right) e^{j\beta_m z} &= \sum_{m=1}^{2} \left(jA_m\beta_m \hat{\mathbf{z}} \times \boldsymbol{h}_m + \frac{dA_m}{dz} \hat{\mathbf{z}} \times \boldsymbol{h}_m \right) e^{j\beta_m z} \end{aligned} \tag{30.4}$$

Now multiple the two equations in (30.4) by $\boldsymbol{h}_n^* e^{-j\beta_n z}$ and $\boldsymbol{e}_n^* e^{-j\beta_n z}$ respectively

$$\sum_{m=1}^{2}\left(-\left(\nabla_\perp\times\boldsymbol{e}_m\right)\cdot\boldsymbol{h}_n^*+j\omega\mu\boldsymbol{h}_m\cdot\boldsymbol{h}_n^*\right)e^{j(\beta_m-\beta_n)z}=j\beta\sum_{m=1}^{2}A_m\left(\hat{\mathbf{z}}\times\boldsymbol{e}_m\right)\cdot\boldsymbol{h}_n^*e^{j(\beta_m-\beta_n)z}+\sum_{m,n}\frac{dA_m}{dz}\left(\hat{\mathbf{z}}\times\boldsymbol{e}_m\right)\cdot\boldsymbol{h}_n^*e^{j(\beta_m-\beta_n)z}$$

$$\sum_{m=1}^{2}\left(-\left(\nabla_\perp\times\boldsymbol{h}_m\right)\cdot\boldsymbol{e}_n^*-j\omega\varepsilon_0\varepsilon_r\boldsymbol{e}_m\cdot\boldsymbol{e}_n^*\right)e^{j(\beta_m-\beta_n)z}=j\beta\sum_{m=1}^{2}A_m\left(\hat{\mathbf{z}}\times\boldsymbol{h}_m\right)\cdot\boldsymbol{e}_n^*e^{j(\beta_m-\beta_n)z}+\sum_{m,n}\frac{dA_m}{dz}\left(\hat{\mathbf{z}}\times\boldsymbol{h}_m\right)\cdot\boldsymbol{e}_n^*e^{j(\beta_m-\beta_n)z}$$

(30.5)

and subtract the second line from the first one

$$\sum_{m=1}^{2}A_m\left[\left(\nabla_\perp\times\boldsymbol{h}+j\omega\varepsilon_0\varepsilon_r\boldsymbol{e}\right)\cdot\boldsymbol{e}_n^*-\left(\nabla_\perp\times\boldsymbol{e}-j\omega\mu\boldsymbol{h}\right)\cdot\boldsymbol{h}_n^*-j\beta\hat{\mathbf{z}}\cdot\left(\boldsymbol{e}_m\times\boldsymbol{h}_n^*+\boldsymbol{e}_n^*\times\boldsymbol{h}_m\right)\right]e^{j(\beta_m-\beta_n)z}=$$

$$=\sum_{m=1}^{2}\frac{dA_m}{dz}\hat{\mathbf{z}}\cdot\left(\boldsymbol{e}_m\times\boldsymbol{h}_n^*+\boldsymbol{e}_n^*\times\boldsymbol{h}_m\right)e^{j(\beta_m-\beta_n)z}$$

(30.6)

Next, consider that dielectric permittivity is perturbed as $\varepsilon_r+\delta\varepsilon_r$, which immediately cancel all the terms on the l.h.s. except the perturbation

$$\sum_{m=1}^{2}A_m\,j\omega\varepsilon_0\delta\varepsilon_r\boldsymbol{e}\cdot\boldsymbol{e}_n^*e^{j(\beta_m-\beta_n)z}=\sum_{m=1}^{2}\frac{dA_m}{dz}\hat{\mathbf{z}}\cdot\left(\boldsymbol{e}_m\times\boldsymbol{h}_n^*+\boldsymbol{e}_n^*\times\boldsymbol{h}_m\right)e^{j(\beta_m-\beta_n)z}\tag{30.7}$$

We can now integrate (30.7) over the waveguide area and use the orthogonality of the modes Eq. 29.67

$$\int_{-\infty}^{\infty}\int_{-\infty}^{\infty}(\boldsymbol{e}_m\times\boldsymbol{h}_n^*+\boldsymbol{e}_n^*\times\boldsymbol{h}_m)_z\,dxdy=4\delta_{mn}\tag{30.8}$$

To keep just one, m=n term on the r.h.s.

$$j\omega\varepsilon_0\sum_{m=1}^{2}\int\int A_m\boldsymbol{e}^*{}_n\cdot\delta\varepsilon_r\boldsymbol{e}_m dxdye^{j(\beta_m-\beta_n)z}=\frac{dA_n}{dz}\int\int\hat{\mathbf{z}}\cdot\left(\boldsymbol{e}_m\times\mathbf{h}_n^*+\boldsymbol{e}_n^*\times\mathbf{h}_m\right)dxdy\tag{30.9}$$

Introduce the matrix of coupling coefficients with diagonal elements

$$\kappa_{nn}=\frac{\omega\varepsilon_0\int\int\boldsymbol{e}_n\cdot\delta\varepsilon_r(x,y)\boldsymbol{e}_n^*dxdy}{\int\int\hat{\mathbf{z}}\cdot\left[\boldsymbol{e}_n\times\boldsymbol{h}_n^*+\boldsymbol{e}_n^*\times\boldsymbol{h}_n\right]dxdy}=\frac{\omega}{4c\eta_0}\int\int\boldsymbol{e}_n\cdot\delta\varepsilon_r(x,y)\boldsymbol{e}_n^*dxdy=\frac{\omega}{c}\delta n_{eff,n}=\delta\beta_n\tag{30.10}$$

where we have used Eq. (29.101) , and off-diagonal elements

$$\kappa_{nm}=\kappa_{mn}^*=\frac{\omega\varepsilon_0\int\int\boldsymbol{e}_n\cdot\delta\varepsilon_r(x,y)\boldsymbol{e}_m^*dxdy}{\int\int\hat{\mathbf{z}}\cdot\left[\boldsymbol{e}_n\times\boldsymbol{h}_n^*+\boldsymbol{e}_n^*\times\boldsymbol{h}_n\right]dxdy}=\frac{\omega}{4c\eta_0}\int\int\boldsymbol{e}_n\cdot\delta\varepsilon_r(x,y)\boldsymbol{e}_m^*dxdy\tag{30.11}$$

Now the coupled equations (and there are two of them, since we can change indices n and m in (30.9) become

$$\frac{dA_1}{dz} = j\kappa_{11}A_1 + j\kappa_{12}A_2 e^{j(\beta_2-\beta_1)z}$$
$$\frac{dA_2}{dz} = j\kappa_{22}A_2 + j\kappa_{21}A_1 e^{-j(\beta_2-\beta_1)z} \tag{30.12}$$

Note that $\kappa_{12} = \kappa_{21}^*$. Usually though we select $\mathbf{e}$ and $\mathbf{h}$ to be real and $\kappa_{12} = \kappa_{21}$. Next we get rid of diagonal terms by introducing new variables

$$A_1 = A_1' e^{j\delta\beta_1 z}$$
$$A_2 = A_2' e^{j\delta\beta_2 z} \tag{30.13}$$

When (30.13)substituted into (30.12) we obtain

$$\frac{dA_1'}{dz} + j\delta\beta_1 A_1' = j\delta\beta_1 A_1' + j\kappa_{12}A_2' e^{j(\beta_2-\beta_1+\delta\beta_2-\delta\beta_1)z}$$
$$\frac{dA_2'}{dz} + j\delta\beta_2 A_2' = j\delta\beta_2 A_2' + j\kappa_{21}A_1' e^{-j(\beta_2-\beta_1+\delta\beta_2-\delta\beta_1)z} \tag{30.14}$$

Perform cancellation and introduce new wavevector mismatch

$$\Delta\beta = \beta_2 + \delta\beta_2 - \beta_1 - \delta\beta_1 \tag{30.15}$$

We can also drop the primes because usually we are not interested in phases of the fields, only in their amplitudes. So we finally obtain a well-known system of equations

$$\frac{dA_1}{dz} = j\kappa_{12}A_2 e^{j\Delta\beta z}$$
$$\frac{dA_2}{dz} = j\kappa_{21}A_1 e^{-j\Delta\beta z} \tag{30.16}$$

This way one can perform mode conversion between the identical polarizations of different ones, i.e. TE to TM mode conversion. For that one need to take into account tensor character of perturbation

$$\delta\varepsilon_r = \begin{pmatrix} \delta\varepsilon_{r,11} & \delta\varepsilon_{r,12} & \delta\varepsilon_{r,13} \\ \delta\varepsilon_{r,21} & \delta\varepsilon_{r,22} & \delta\varepsilon_{r,23} \\ \delta\varepsilon_{r,31} & \delta\varepsilon_{r,32} & \delta\varepsilon_{r,33} \end{pmatrix} \tag{30.17}$$

If the direction of propagation is z, TE wave is y polarized and TM wave is x-polarized, from (30.11) one gets

$$\kappa_{TEn\to TMm} = \frac{\omega}{4c\eta_0}\int\int e_{yn}^{TE}\delta\varepsilon_{r21}(x,y)e_{xm}^{TM*}dxdy \tag{30.18}$$

This way one can build polarization converter. Not that for the well confined waveguides or when indices in core and cladding are close and the material is isotropic

$$\kappa_{12} \sim \frac{\omega}{2n_{eff}c}\frac{\int\int \boldsymbol{e}_1 \cdot \delta\varepsilon_r(x,y)\boldsymbol{e}_2^* dxdy}{\sqrt{\int\int e_1^{\,2}dxdy}\sqrt{\int\int e_2^{\,2}dxdy}} \sim \frac{\omega}{n_{eff}c}\frac{\int\int e_1 \delta n(x,y) e_2^* dxdy}{\sqrt{\int\int e_1^{\,2}dxdy}\sqrt{\int\int e_2^{\,2}dxdy}} \tag{30.19}$$

Coupling between two waveguides

Previously we have looked at coupling two modes within one waveguide. Now consider two waveguides with (for now) one mode in each as shown in Fig.30.2

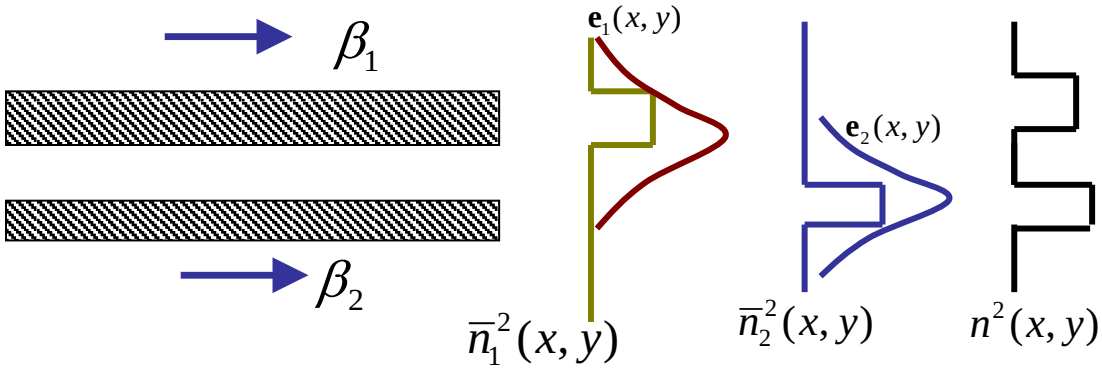

Figure 30.2 Coupling between two waveguides

The profile of the dielectric constant (refractive index squared) can be split into two parts

$$n^2(x,y) = \bar{n}_1^2(x,y) + \left[n^2(x,y) - \bar{n}_1^2(x,y)\right] = \bar{n}_1^2(x,y) + \delta n_{21}^2(x,y)$$
$$\text{or} \tag{30.20}$$
$$n^2(x,y) = \bar{n}_2^2(x,y) + \left[n^2(x,y) - \bar{n}_2^2(x,y)\right] = \bar{n}_2^2(x,y) + \delta n_{12}^2(x,y)$$

where $\bar{n}_{1,2}^2(x,y)$ is the dielectric constant profile for one of the waveguide in the absence of the other and $\delta n_{12}^2(x,y)$ or $\delta n_{21}^2(x,y)$ is the perturbation. The two modes in the uncoupled solutions have propagation constants $\beta_{1,2}$ and the mode shapes that are solutions of the Maxwell's equations for each waveguide,

$$\begin{aligned}\nabla_\perp \times \boldsymbol{e}_{1,2} + j\beta_{1,2}\hat{\mathbf{z}}\times\boldsymbol{e}_{1,2} &= j\omega\mu\boldsymbol{h}_{1,2}\\ \nabla_\perp \times \boldsymbol{h}_{1,2} + j\beta_{1,2}\hat{\mathbf{z}}\times\boldsymbol{h}_{1,2} &= -j\omega\varepsilon_0\bar{n}_{1,2}^2(x,y)\boldsymbol{h}_{1,2}\end{aligned} \tag{30.21}$$

Once again, we look for a solution (30.1) which upon substitution into (30.2) yields

$$\begin{aligned}\sum_{m=1}^{2} A_m\left(-\nabla_\perp\times\boldsymbol{e}_m + j\omega\mu\boldsymbol{h}_m\right)e^{j\beta_m z} &= \sum_{m=1}^{2}\left(jA_m\beta_m\hat{\mathbf{z}}\times\boldsymbol{e}_m + \frac{dA_m}{dz}\hat{\mathbf{z}}\times\boldsymbol{e}_m\right)e^{j\beta_m z}\\ \sum_{m=1}^{2} A_m\left(-\nabla_\perp\times\boldsymbol{h}_m - j\omega\varepsilon_0 n^2(x,y)\boldsymbol{e}_m\right)e^{j\beta_m z} &= \sum_{m=1}^{2}\left(jA_m\beta_m\hat{\mathbf{z}}\times\boldsymbol{h}_m + \frac{dA_m}{dz}\hat{\mathbf{z}}\times\boldsymbol{h}_m\right)e^{j\beta_m z}\end{aligned} \tag{30.22}$$

Next we can substitute $n^2(x,y) = \overline{n}_m^2(x,y) + \delta n_{nm}^2(x,y)$ use (30.21) to cancel most of the terms and be left with

$$\begin{aligned} 0 &= \sum_{m=1}^{2} \left(\frac{dA_m}{dz} \hat{\mathbf{z}} \times \boldsymbol{e}_m \right) e^{j\beta_m z} \\ \sum_{m=1}^{2} A_m \left(-j\omega\varepsilon_0 \delta n_{nm}^2(x,y) \boldsymbol{e}_m \right) e^{j\beta_m z} &= \sum_{m=1}^{2} \left(\frac{dA_m}{dz} \hat{\mathbf{z}} \times \boldsymbol{h}_m \right) e^{j\beta_m z} \end{aligned} \tag{30.23}$$

Following the well-trodden path we dot-multiply two equations in (30.23) by $\boldsymbol{h}_n^* e^{-j\beta_n z}$ and $\boldsymbol{e}_n^* e^{-j\beta_n z}$ respectively to obtain

$$\begin{aligned} 0 &= \sum_{m,n} \frac{dA_m}{dz} \left(\hat{\mathbf{z}} \times \boldsymbol{e}_m \right) \cdot \boldsymbol{h}_n^* e^{j(\beta_m - \beta_n) z} \\ \sum_{m=1}^{2} A_m \left(-j\omega\varepsilon_0 \boldsymbol{e}_n^* \delta n_{nm}^2(x,y) \boldsymbol{e}_m \right) e^{j(\beta_m - \beta_n) z} &= \sum_{m=1}^{2} \frac{dA_m}{dz} \left(\hat{\mathbf{z}} \times \boldsymbol{h}_m \right) \cdot \boldsymbol{e}_n^* e^{j(\beta_m - \beta_n) z} \end{aligned} \tag{30.24}$$

then perform subtraction

$$j\omega\varepsilon_0 \sum_{m=1}^{2} A_m \left(\boldsymbol{e}_n^* \delta n_{nm}^2(x,y) \boldsymbol{e}_m \right) e^{j(\beta_m - \beta_n) z} = \sum_{m=1}^{2} \frac{dA_m}{dz} \hat{\mathbf{z}} \cdot \left(\boldsymbol{e}_m \times \boldsymbol{h}_n^* + \boldsymbol{e}_n^* \times \boldsymbol{h}_m \right) e^{j(\beta_m - \beta_n) z} \tag{30.25}$$

and finally integrate over the area of cross-section

$$\begin{aligned} & j\omega\varepsilon_0 A_1 \int\int \boldsymbol{e}_1^* \delta n_{12}^2(x,y) \boldsymbol{e}_1 dxdy + j\omega\varepsilon_0 A_2 \int\int \boldsymbol{e}_1^* \delta n_{21}^2(x,y) \boldsymbol{e}_2 dxdy e^{j(\beta_2 - \beta_1) z} = \\ &= \frac{dA_1}{dz} \int\int \hat{\mathbf{z}} \cdot \left(\boldsymbol{e}_1 \times \boldsymbol{h}_1^* + \boldsymbol{e}_1^* \times \boldsymbol{h}_1 \right) dxdy + \frac{dA_2}{dz} \int\int \hat{\mathbf{z}} \cdot \left(\boldsymbol{e}_1 \times \boldsymbol{h}_2^* + \boldsymbol{e}_2^* \times \boldsymbol{h}_1 \right) e^{j(\beta_2 - \beta_1) z} \end{aligned} \tag{30.26}$$

Now, the first integral on the r.h.s. is, according to normalization condition (29.101) is equal to 4, but the second integral is not equal to zero because two mode of isolated waveguides are not orthogonal to each other. So, now we introduce coupling coefficients

$$\begin{aligned} \kappa_{11} &= \frac{j\omega\varepsilon_0 \int\int \boldsymbol{e}_1 \cdot \delta n_{21}^2(x,y) \boldsymbol{e}_1^* dxdy}{\int\int \hat{\mathbf{z}} \cdot \left[\boldsymbol{e}_1 \times \boldsymbol{h}_1^* + \boldsymbol{e}_1^* \times \boldsymbol{h}_1 \right] dxdy} = \frac{\omega}{4c\eta_0} \int\int \boldsymbol{e}_1 \cdot \delta n_{12}^2(x,y) \boldsymbol{e}_1^* dxdy \\ \kappa_{12} &= \frac{\omega\varepsilon_0 \int\int \boldsymbol{e}_1 \cdot \delta n_{12}^2(x,y) \boldsymbol{e}_2^* dxdy}{\int\int \hat{\mathbf{z}} \cdot \left[\boldsymbol{e}_1 \times \boldsymbol{h}_1^* + \boldsymbol{e}_1^* \times \boldsymbol{h}_1 \right] dxdy} = \frac{\omega}{4c\eta_0} \int\int \boldsymbol{e}_1 \cdot \delta n_{12}^2(x,y) \boldsymbol{e}_2^* dxdy \end{aligned} \tag{30.27}$$

and the modal overlap

$$\sigma = \frac{\int\int \hat{\mathbf{z}} \cdot \left[\boldsymbol{e}_1 \times \boldsymbol{h}_2^* + \boldsymbol{e}_2^* \times \boldsymbol{h}_1 \right] dxdy}{\int\int \hat{\mathbf{z}} \cdot \left[\boldsymbol{e}_1 \times \boldsymbol{h}_1^* + \boldsymbol{e}_1^* \times \boldsymbol{h}_1 \right] dxdy} = \frac{\int\int \hat{\mathbf{z}} \cdot \left[\boldsymbol{e}_2 \times \boldsymbol{h}_1^* + \boldsymbol{e}_1^* \times \boldsymbol{h}_2 \right] dxdy}{\int\int \hat{\mathbf{z}} \cdot \left[\boldsymbol{e}_1 \times \boldsymbol{h}_1^* + \boldsymbol{e}_1^* \times \boldsymbol{h}_1 \right] dxdy} << 1 \tag{30.28}$$

Then the coupled mode equations are

$$\frac{dA_1}{dz}+\sigma\frac{dA_2}{dz}e^{j\Delta\beta z}=j\kappa_{11}A_1+j\kappa_{12}A_2e^{j\Delta\beta z}$$
$$\frac{dA_2}{dz}+\sigma\frac{dA_1}{dz}e^{-j\Delta\beta z}=j\kappa_{22}A_2+j\kappa_{21}A_1e^{-j\Delta\beta z} \quad (30.29)$$

where $\Delta\beta=\beta_2-\beta_1$. What we do next is express dA_2/dz from the second equation and substitute it into the first one. And do the same for dA_1/dz -taking it from the first equation and substituting into the second one

$$\frac{dA_1}{dz}+\sigma\left[j\kappa_{22}A_2+j\kappa_{21}A_1e^{-j\Delta\beta z}-\sigma\frac{dA_1}{dz}e^{-j\Delta\beta z}\right]e^{j\Delta\beta z}=j\kappa_{11}A_1+j\kappa_{12}A_2e^{j\Delta\beta z}$$
$$\frac{dA_2}{dz}+\sigma\left[j\kappa_{11}A_1+j\kappa_{12}A_2e^{j\Delta\beta z}-\sigma\frac{dA_2}{dz}e^{j\Delta\beta z}\right]e^{-j\Delta\beta z}=j\kappa_{22}A_2+j\kappa_{21}A_1e^{-j\Delta\beta z} \quad (30.30)$$

Now we can combine the terms and introduce new, primed coupling coefficients

$$\frac{dA_1}{dz}=j\frac{\kappa_{11}-\sigma\kappa_{21}}{1-\sigma^2}A_1+j\frac{\kappa_{12}-\sigma\kappa_{22}}{1-\sigma^2}A_2e^{j\Delta\beta z}=j\kappa_{11}^{'}A_1+j\kappa_{12}^{'}A_2e^{j\Delta\beta z}$$
$$\frac{dA_2}{dz}=j\frac{\kappa_{22}-\sigma\kappa_{12}}{1-\sigma^2}A_2+j\frac{\kappa_{21}-\sigma\kappa_{11}}{1-\sigma^2}A_1e^{-j\Delta\beta z}=j\kappa_{22}^{'}A_2+j\kappa_{21}^{'}A_1e^{j\Delta\beta z} \quad (30.31)$$

So, now the equations (30.31) look precisely like (30.12), and we already know how to get rid of the diagonal terms by modifying propagation constants, so, after dropping the primes we arrive at

$$\frac{dA_1}{dz}=j\kappa_{12}A_2e^{j\Delta\beta z}$$
$$\frac{dA_2}{dz}=j\kappa_{21}A_1e^{-j\Delta\beta z} \quad (30.32)$$

Directional coupler

Let us now consider two identical waveguides as shown in Fig.30.3a. The coupled equations (30.32) under condition $\Delta\beta=0$ become

$$\frac{dA_1}{dz}=j\kappa A_2$$
$$\frac{dA_2}{dz}=j\kappa A_1 \quad (30.33)$$

With the obvious solution

$$A_1(z)=C_1\cos(\kappa z)+C_2\sin(\kappa z)$$
$$A_2(z)=-j\kappa^{-1}\frac{dA_1}{dz}=jC_1\sin(\kappa z)-jC_2\cos(\kappa z) \quad (30.34)$$

Plugging in boundary conditions at z=0 we get

$$A_1(0) = C_1$$
$$A_2(0) = -jC_2 \tag{30.35}$$

And the solution is

$$A_1(z) = A_1(0)\cos(\kappa z) + jA_2(0)\sin(\kappa z)$$
$$A_2(z) = jA_1(0)\sin(\kappa z) + A_2(0)\cos(\kappa z), \tag{30.36}$$

or, in matrix from,

$$\begin{pmatrix} A_1(z) \\ A_2(z) \end{pmatrix} = \begin{pmatrix} \cos(\kappa z) & j\sin(\kappa z) \\ j\sin(\kappa z) & \cos(\kappa z) \end{pmatrix} \begin{pmatrix} A_1(0) \\ A_2(0) \end{pmatrix} \tag{30.37}$$

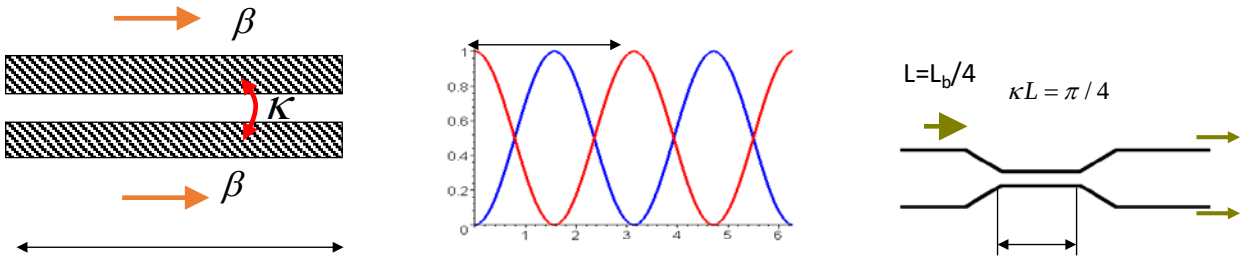

Figure 30.3 (a) waveguides in a directional coupler (b) Characteristics of directional coupler (c) 3-dB coupler.

More often than not there is no input in one of the waveguides

$$A_1(0) = A_0; A_2(0) = 0 \tag{30.38}$$

and the solution becomes

$$A_1(z) = A_0\cos(\kappa z)$$
$$A_2(z) = jA_0\sin(\kappa z) \tag{30.39}$$

and since according to (29.66) power, $P_m = |A_m|^2$ the power transfer between the waveguides is described as

$$P_1(z) = P_0\cos^2(\kappa z);$$
$$P_2(z) = P_0\sin^2(\kappa z); \tag{30.40}$$

as shown in Fig.30.3b. We can introduce the *beat length* as

$$L_b = \pi\kappa^{-1} \tag{30.41}$$

which is the full period of power transfer

$$\begin{pmatrix} A_1(L_b) \\ A_2(L_b) \end{pmatrix} = \begin{pmatrix} -1 & 0 \\ 0 & -1 \end{pmatrix} \begin{pmatrix} A_1(0) \\ A_2(0) \end{pmatrix} = -\begin{pmatrix} A_1(0) \\ A_2(0) \end{pmatrix} \tag{30.42}$$

Then, if the one chooses the coupling length $L = L_b / 4$ as shown in Fig.30.3c, then

$$\begin{pmatrix} A_1(L) \\ A_2(L) \end{pmatrix} = \begin{pmatrix} \frac{1}{\sqrt{2}} & j\frac{1}{\sqrt{2}} \\ j\frac{1}{\sqrt{2}} & \frac{1}{\sqrt{2}} \end{pmatrix} \begin{pmatrix} A_1(0) \\ A_2(0) \end{pmatrix} = \frac{1}{\sqrt{2}} \begin{pmatrix} A_1(0) + jA_2(0) \\ jA_1(0) + A_2(0) \end{pmatrix} \tag{30.43}$$

and if only one input port has input power in it (30.38)t the output power will be evenly split between two output ports

$$P_1(L) = P_2(L) = P_0 / 2 \tag{30.44}$$

Hence such coupler is called a *3-dB coupler*.

Optical hybrids in coherent communications.

In coherent optical communications one needs to detect phase $\varphi_s(t)$ of the signal

$$E_s = A_s e^{j\varphi_s(t)} e^{-j\omega t} + c.c. \tag{30.45}$$

The phase contains all the information that is being transmitted. Example of of phase modulation, shown in Fig.30.4a is BPSK-binary phase shift keying where the values of 1 and 0 correspond to the phase of 0 and 180 digress respectively. In the quadrature phase shift keying(QPSK) modulation format two bits are encoded as shown in Fig.30.4b with four value corresponding to four different phases separated by 90 degrees. For BPSK ad QPSK the amplitude of the signal remains unchanged. There are many reasons while phase (or frequency) modulation is more robust than amplitude modulation of the signal.

Now, to detect the phase one has to compare it to the phase of a known signal, called local oscillator,

$$E_{LO} = A_{LO} e^{j\varphi_{LO}} e^{-j\omega t} + c.c. \tag{30.46}$$

When the signal and local oscillator are combined on the detector as shown in Fig.30.4c, the detected optical power is

$$P(t) \sim \left\langle (E_s + E_{LO})^2 \right\rangle_t = A_s^2 + A_{LO}^2 + A_s e^{j\varphi_s(t)} A_{LO} e^{-j\varphi_{LO}} + A_s e^{-j\varphi_s(t)} A_{LO} e^{+j\varphi_{LO}} = A_s^2 + A_{LO}^2 + 2A_s A_{LO} \cos(\varphi_s(t) - \varphi_{LO}) \tag{30.47}$$

The phase of LO can be taken as 0 and the current of the photodetector is

$$i_s(t) \sim \eta P_s + \eta P_{LO} + 2\eta\sqrt{P_s P_{LO}} \cos\varphi_s(t) \tag{30.48}$$

where η is the responsivity of the detector (measured in A/W) . Since the signal power P_s is low and the LO power P_{LO} is much higher, one can see that the information containing AC current $i_s(t) = 2\eta\sqrt{P_s P_{LO}}\cos\varphi_s(t)$ is amplified (relative to ηP_s) however the current due to LO, $i_{LO} = \eta P_{LO}$ is much stronger than $i_s(t)$ - the LO current can saturate the amplifiers and also its relative intensity noise (RIN) deteriorates signal to noise ratio.

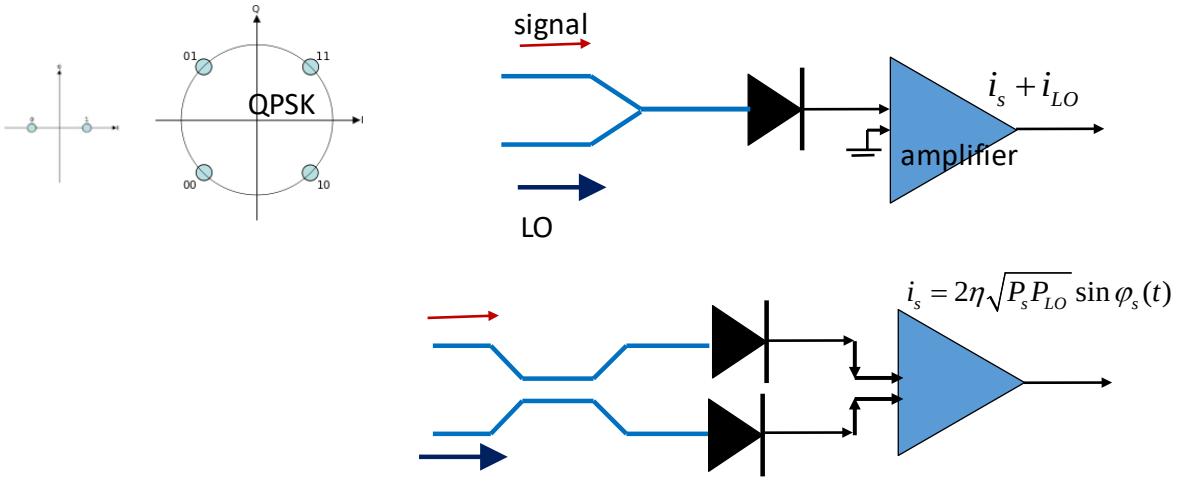

Figure 30.4. (a) BPSK signal (b) QPSK signal (c) Coherent detection with local oscillator (d) Coherent detection with optical hybrid and balanced detector.

To remedy the situation one needs to cancel the large $i_{LO} = \eta P_{LO}$ current and its RIN. That is done using an optical hybrid, which is a 3dB coupler and two identical (balanced) detectors as shown in Fig. 30.4d. The optical field in the upper and lower arms of the balanced detector are

$$E_1 = \frac{1}{\sqrt{2}} A_s e^{j\varphi_s(t)} e^{-j\omega t} + j\frac{1}{\sqrt{2}} A_{LO} e^{-j\omega t} + c.c.$$
$$E_2 = j\frac{1}{\sqrt{2}} A_s e^{j\varphi_s(t)} e^{-j\omega t} + \frac{1}{\sqrt{2}} A_{LO} e^{-j\omega t} + c.c. = j[\frac{1}{\sqrt{2}} A_s e^{j\varphi_s(t)} e^{-j\omega t} - j\frac{1}{\sqrt{2}} A_{LO} e^{-j\omega t}] + c.c.$$

(30.49)

The optical powers on two detectors are

$$P_1 = \left\langle E_1^2 \right\rangle_t = \frac{1}{2}A_s^2 + \frac{1}{2}A_{LO}^2 - jA_s e^{j\varphi_s(t)} A_{LO} + jA_s e^{-j\varphi_s(t)} A_{LO} = \frac{1}{2}P_s + \frac{1}{2}P_{LO} + \sqrt{P_s P_{LO}}\sin\varphi_s(t)$$
$$P_2 = \left\langle E_2^2 \right\rangle_t = \frac{1}{2}A_s^2 + \frac{1}{2}A_{LO}^2 + jA_s e^{j\varphi_s(t)} A_{LO} - jA_s e^{-j\varphi_s(t)} A_{LO} = \frac{1}{2}P_s + \frac{1}{2}P_{LO} - \sqrt{P_s P_{LO}}\sin\varphi_s(t)$$

(30.50)

If the detectors have identical responsivities (balanced detector) subtracting the two currents cancels all currents except the signal current All the RIN gets cancelled.

Mach Zehnder Interferometer (MZI)

MZI in its integrated implementation consists of two 3dB couplers with two waveguides connecting them. One of the waveguides (upper arm) is longer by a length ΔL, as shown in Fig.30.5a. The phase delay between two arms is

$$\Delta\Phi = \beta\Delta L = n_{eff} k_0 \Delta L \tag{30.51}$$

Using matrix approach (30.43)we can find the relation between input and output field

$$\begin{pmatrix} A_{1,out} \\ A_{2,out} \end{pmatrix} = \begin{pmatrix} \frac{1}{\sqrt{2}} & j\frac{1}{\sqrt{2}} \\ j\frac{1}{\sqrt{2}} & \frac{1}{\sqrt{2}} \end{pmatrix} \begin{pmatrix} e^{j\Delta\Phi/2} & 0 \\ 0 & e^{-j\Delta\Phi/2} \end{pmatrix} \begin{pmatrix} \frac{1}{\sqrt{2}} & j\frac{1}{\sqrt{2}} \\ j\frac{1}{\sqrt{2}} & \frac{1}{\sqrt{2}} \end{pmatrix} \begin{pmatrix} A_{1,in} \\ A_{2,in} \end{pmatrix} =$$

$$= \begin{pmatrix} \frac{1}{\sqrt{2}} & j\frac{1}{\sqrt{2}} \\ j\frac{1}{\sqrt{2}} & \frac{1}{\sqrt{2}} \end{pmatrix} \begin{pmatrix} \frac{e^{j\Delta\Phi/2}}{\sqrt{2}} & j\frac{e^{j\Delta\Phi/2}}{\sqrt{2}} \\ j\frac{e^{-j\Delta\Phi/2}}{\sqrt{2}} & \frac{e^{-j\Delta\Phi/2}}{\sqrt{2}} \end{pmatrix} \begin{pmatrix} A_{1,in} \\ A_{2,in} \end{pmatrix} = \begin{pmatrix} j\sin(\Delta\Phi/2) & j\cos(\Delta\Phi/2) \\ j\cos(\Delta\Phi/2) & -j\sin(\Delta\Phi/2) \end{pmatrix} \begin{pmatrix} A_{1,in} \\ A_{2,in} \end{pmatrix}$$

(30.52)

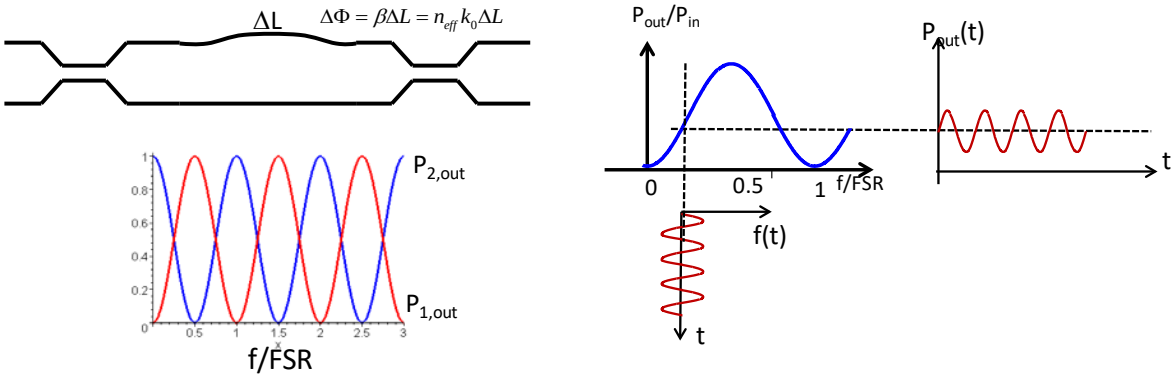

Figure 30.5. (a) MZI schematics (b) MZI output vs. frequency characteristics (c) Unbalanced MZI as frequency discriminator (detector)

Now, if $A_{1,in} = A_0$ and $A_{2,in} = 0$ we obtain the output power in two branches

$$\begin{aligned} P_{1,out} &= P_0 \sin^2(\Delta\Phi/2) = P_0 \sin^2(\pi n_{eff} \Delta L f / c) = P_0 \sin^2(\pi f / FSR); \\ P_{2,out} &= P_0 \cos^2(\Delta\Phi/2) = P_0 \cos^2(\pi n_{eff} \Delta L f / c) = P_0 \cos^2(\pi f / FSR); \end{aligned} \tag{30.53}$$

Where we introduced free spectral range as

$$FSR = c / n_{eff} \Delta L \tag{30.54}$$

The output characteristics is shown in Fig.30.5b. The unbalanced MZi can act as a sensor (when effective index changes) or as a frequency discriminator – which transforms frequency modulation $f(t)$ into intensity modulation $P(t)$ as shown in Fig.30.5.c

One can also use MZI as an optical interleaver. Consider the WDM (wavelength division multiplexed) consisting of a number of independent channels centered on the frequencies $f_n = f_0 + n\Delta f$. If the FSR if the MZi is chosen as $FSR = 2\Delta f$ and $f_0 = m \times FSR$ we have

$$P_{1,out}(f_n) = P_0 \sin^2(\pi f_n / FSR) = P_0 \sin^2(\pi + \pi n/2) = P_0 \sin^2(\pi n/2)$$
$$P_{2,out}(f_n) = P_0 \cos^2(\pi f_n / FSR) = P_0 \cos^2(\pi + \pi n/2) = P_0 \cos^2(\pi n/2) \quad (30.55)$$

So, all the odd channels end up in the upper branch and the even one in the lower branch and interleaver acts as a demultiplexer as shown in Fig.30.6a . Obviously it also works in reverse, as a multiplexer, combining the independently modulated channels into one output. Cascading N interleavers with different FSRs as shown in Fig.30.6b allows one fully demultiplex 2^N channels.

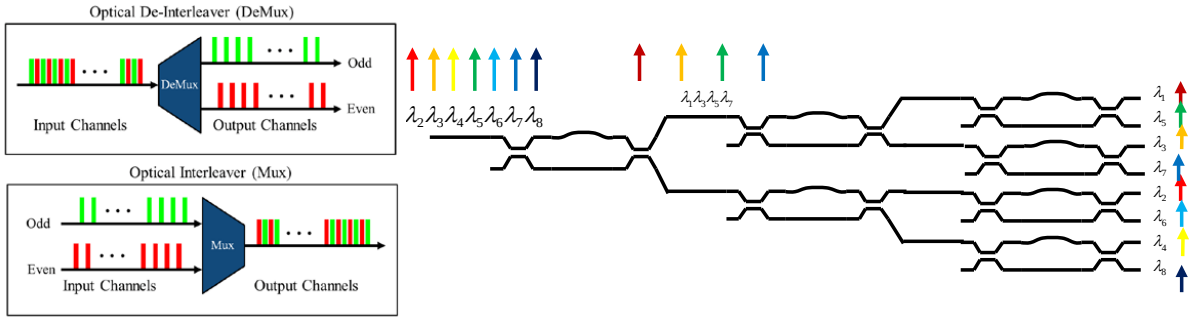

Figure 30.6 (a) MZI Interleaver working as DEMUX (de-multiplexer) and MUX (multiplexer). (b) Cascaded interleaver

MZI Electro-Optic Modulator

Previously, in Chapter 24 we have considered electro-optic modulators based on coupling between two polarization states. But coupling between two polarization states considered there and coupling between two waveguides are described by the same equations r matrices. Therefore, one can use integrated MZI as a modulator as shown in Fig.30.7. When voltage $V(t)$ is applied to the left and right electrodes, while the central electrode is grounded, the electric fields in two arms have opposite signs (so-called push-pull configuration). The change of the effective index in the waveguide is

$$n_{eff,1(2)}(V) = n_{eff,0} + \frac{1}{2} n_{eff,0}^3 r_{eff} E_{eff,1(2)} = n_{eff,0} \pm \frac{1}{2} n_{eff,0}^3 r_{eff} V / d_{eff} \quad (30.56)$$

where r_{eff} is effective Pockels coefficient (considering polarization of the mode and field direction) and d_{eff} is the effective width which takes into account the fact that the field between the electrodes is not uniform and also penetrates outside of the gap.

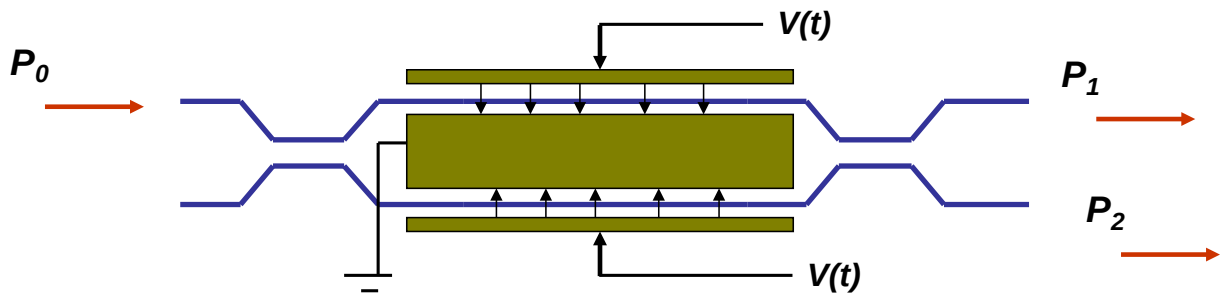

Figure 30.7 Integrated MZI electro-optic modulator

The phase shift between two arms is

$$\Delta\Phi_{12} = k_0 L(n_{eff,1} - n_{eff,2}) = k_0 L n_{eff,0}^3 r_{eff} V / d_{eff} = \pi V / V_\pi \tag{30.57}$$

where half-wave voltage is

$$V_\pi = \frac{\pi}{k_0 n_{eff,0}^3 r_{eff} L / d_{eff}} \tag{30.58}$$

The output powers are

$$\begin{aligned} P_{1,out}(t) &= P_0 \sin^2(\Delta\Phi/2) = P_0 \sin^2 \frac{\pi V(t)}{2V_\pi} \\ P_{2,out}(t) &= P_0 \cos^2(\Delta\Phi/2) = P_0 \cos^2 \frac{\pi V(t)}{2V_\pi} \end{aligned} \tag{30.59}$$

This is essentially the same characteristics as in birefringent-based EO modulators of Chapter 24.

Mismatched directional coupler

Let us now return to the general case when propagation constants of two coupled waveguides are different (Fig.30.8a), as in (30.32) which we repeat here

$$\begin{aligned} \frac{dA_1}{dz} &= j\kappa A_2 e^{j\Delta\beta z} \\ \frac{dA_2}{dz} &= j\kappa A_1 e^{-j\Delta\beta z} \end{aligned} \tag{30.60}$$

Perform a familiar substitution

$$\begin{aligned} A_1 &= A_1' e^{j\Delta\beta z/2} \\ A_2 &= A_2' e^{-j\Delta\beta z/2} \end{aligned} \tag{30.61}$$

and obtain

$$\frac{dA_1^{'}}{dz} + j\frac{\Delta\beta}{2}A_1^{'} = j\kappa A_2^{'}$$
$$\frac{dA_2^{'}}{dz} - j\frac{\Delta\beta}{2}A_2^{'} = j\kappa A_1^{'} \tag{30.62}$$

The primes can now be dropped and solution sought as

$$A_{1,2}(z) \sim A_{1,2}^0 e^{j\gamma z} \tag{30.63}$$

Which upon substitution into (30.62) yields

$$j\gamma A_1^0 + j\frac{\Delta\beta}{2}A_1^0 - j\kappa A_2^0 = 0$$
$$j\gamma A_2^0 - j\frac{\Delta\beta}{2}A_2^0 - jA_2^0 = 0 \tag{30.64}$$

Or in matrix form

$$\begin{pmatrix} \gamma + \frac{\Delta\beta}{2} & -\kappa \\ -\kappa & \gamma - \frac{\Delta\beta}{2} \end{pmatrix} \begin{pmatrix} A_1^0 \\ A_2^0 \end{pmatrix} = 0 \tag{30.65}$$

The nontrivial solution of course exists only if the determinant of the matrix is zero and characteristic equation follows

$$\left(\gamma + \frac{\Delta\beta}{2}\right)\left(\gamma - \frac{\Delta\beta}{2}\right) - \kappa^2 = 0; \tag{30.66}$$

with the roots

$$\gamma = \pm\sqrt{\kappa^2 + \frac{\Delta\beta^2}{4}} \tag{30.67}$$

Therefore, the solution of couple equations is

$$A_1(z) = C_1\cos(\gamma z) + C_2\sin(\gamma z)$$
$$A_2(z) = -j\kappa^{-1}\left(\frac{dA_1}{dz} + j\frac{\Delta\beta}{2}\right) = -j\frac{-\gamma C_1 + j\frac{\Delta\beta}{2}C_2}{\kappa}\sin(\gamma z) - j\frac{\gamma C_2 + j\frac{\Delta\beta}{2}C_1}{\kappa}\cos(\gamma z) \tag{30.68}$$

If the boundary conditions are

$$A_1(0) = A_0$$
$$A_2(0) = 0, \tag{30.69}$$

we have

$$C_2 = -j\frac{\Delta\beta}{2\gamma}C_1;\ C_1 = A_0 \tag{30.70}$$

and

$$A_2(z) = -jA_0\frac{-\gamma+\frac{\Delta\beta^2}{4\gamma}}{\kappa}\sin(\gamma z) = jA_0\frac{\gamma^2-\frac{\Delta\beta^2}{4}}{\kappa\gamma}\sin(\gamma z) = jA_0\frac{\kappa}{\gamma}\sin(\gamma z) \tag{30.71}$$

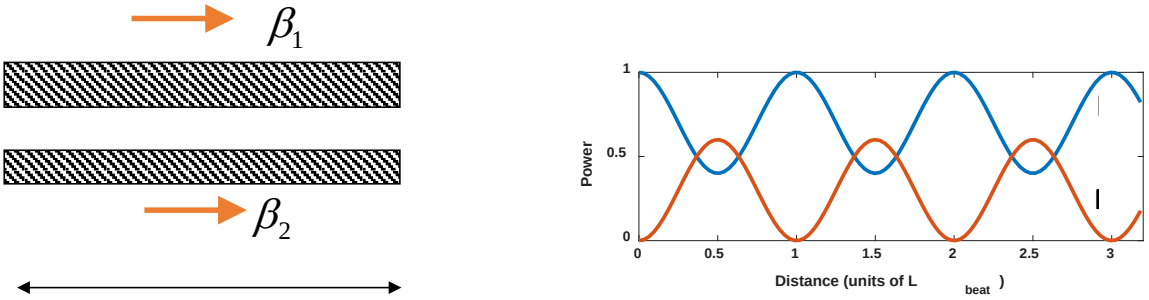

Figure 30.8 (a) Mismatched directional coupler (b) Power vs. length characteristics of it.

For powers we obtain

$$P_2(z) = P_0\frac{\kappa^2}{\kappa^2+\frac{\Delta\beta^2}{4}}\sin^2\gamma z$$
$$P_1(z) = 1-P_2(z) \tag{30.72}$$

As shown in Fig. 30.8b. The power transfer is no longer complete and the beat length is now shorter compared to the perfectly matched case.

$$L_b = \pi\gamma^{-1} = \frac{\pi}{\sqrt{\kappa^2+\frac{\Delta\beta^2}{4}}} \tag{30.73}$$

Electro-optic modulator based on the directional coupler

One can use directional coupler without anything else to achieve modulation. As shown in Fig. 30.9a, the length of the coupler is half the beat length,

$$L = L_b/2 = \pi/2\kappa \tag{30.74}$$

two coupled waveguides have the same effective index, but when the voltage is applied in push-pull configuration the mismatch appears,

$$\Delta\beta = k_0 n_{eff,0}^3 r_{eff} V/d_{eff} = \frac{\pi}{L}\frac{V}{V_\pi} = 2\kappa\frac{V}{V_\pi} \tag{30.75}$$

According to (30.67)

$$\gamma = \sqrt{\kappa^2 + \frac{\Delta\beta^2}{4}} = \kappa\sqrt{1+\frac{V^2}{V_\pi^2}} = \frac{\pi}{2L}\sqrt{1+\frac{V^2}{V_\pi^2}} \tag{30.76}$$

and then according to (30.72)

$$P_2(L) = P_0\frac{\kappa^2}{\gamma^2}\sin^2\gamma L = P_0\frac{1}{1+\frac{V^2}{V_\pi^2}}\sin^2\frac{\pi}{2}\sqrt{1+\frac{V^2}{V_\pi^2}} \tag{30.77}$$

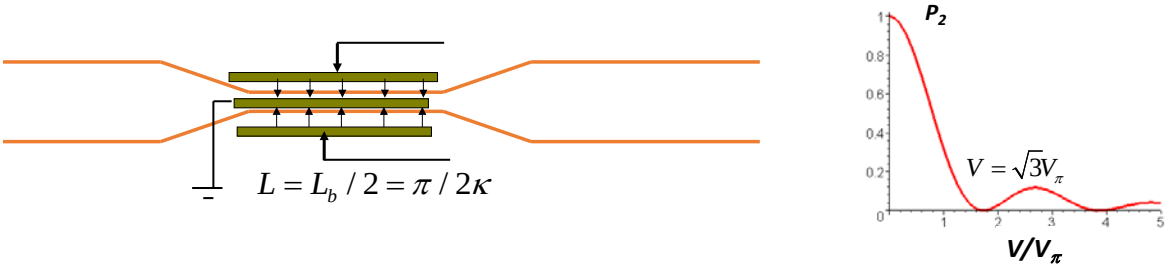

Figure 30.9(a) EO modulator based on directional coupler (b) Switching characteristics of it

The voltage dependence of output power is shown in Fig. 30.9b. The switching voltage is $\sqrt{3}V_\pi$ which is somewhat higher than V_π for MZI modulator, but the advantage of the directional coupler-type modulator is that the response does not oscillate as much as in MZI and as long as $V >> \sqrt{3}V_\pi$ the output is very small

Supermodes.

Let us consider directional coupler shown in Fig.30.10 with two identical waveguides and input into just one of the waveguides,

$$\begin{aligned} &A_1(0) = A_0; A_2(0) = 0 \\ &\beta_1 = \beta_2 = \beta \end{aligned} \tag{30.78}$$

The solution for the amplitudes of two waves is (30.39)

$$\begin{aligned} A_1(z) &= A_0\cos(\kappa z) \\ A_2(z) &= jA_0\sin(\kappa z) \end{aligned} \tag{30.79}$$

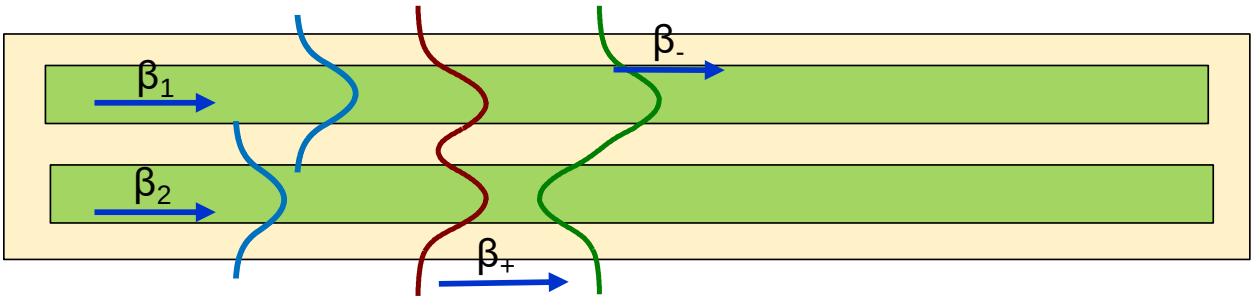

Figure 30.10 Supermodes concept for two identical coupled waveguides

The total electric filed is given by and can be re-worked as

$$\begin{aligned}
&\boldsymbol{E} = A_0 \cos(\kappa z) e^{j\beta z} \boldsymbol{e}_1(x,y) + jA_0 \sin(\kappa z) e^{j\beta z} \boldsymbol{e}_2(x,y) = \\
&= \frac{1}{2} A_0 \left[e^{j(\beta+\kappa)z} \boldsymbol{e}_1(x,y) + e^{j(\beta-\kappa)z} \boldsymbol{e}_1(x,y) + e^{j(\beta+\kappa)z} \boldsymbol{e}_2(x,y) - e^{j(\beta-\kappa)z} \boldsymbol{e}_2(x,y) \right] = \\
&= \frac{1}{2} A_0 e^{j(\beta+\kappa)z} \left[\boldsymbol{e}_1(x,y) + \boldsymbol{e}_2(x,y) \right] + \frac{1}{2} A_0 e^{j(\beta-\kappa)z} \left[\boldsymbol{e}_1(x,y) - \boldsymbol{e}_2(x,y) \right] = \\
&= \frac{A_0}{\sqrt{2}} e^{j\beta_+ z} \boldsymbol{e}_+(x,y) + \frac{A_0}{\sqrt{2}} e^{j\beta_- z} \boldsymbol{e}_-(x,y)
\end{aligned} \tag{30.80}$$

Here we introduced two new "supermodes": a symmetric (even) one

$$\begin{aligned}
&\boldsymbol{e}_+(x,y) = \frac{\boldsymbol{e}_1(x,y) + \boldsymbol{e}_2(x,y)}{\sqrt{2}} \\
&\beta_+ = \beta + \kappa
\end{aligned} \tag{30.81}$$

and an anti-symmetric (odd) one

$$\begin{aligned}
&\boldsymbol{e}_-(x,y) = \frac{\boldsymbol{e}_1(x,y) - \boldsymbol{e}_2(x,y)}{\sqrt{2}} \\
&\beta_- = \beta - \kappa
\end{aligned} \tag{30.82}$$

The amplitudes of these coupled modes do not change, hence they must be the exact solutions of the wave equation.

Now let us consider a more general case when two waveguides have different propagation constants as shown in Fig.30.11. We shall look for a solution

$$\boldsymbol{E} = \sum_{m=1}^{2} C_m \boldsymbol{e}_m(x,y) \cdot e^{j\beta z} \tag{30.83}$$

Where coefficients C_m are constant and not distance dependent as in (30.1), and propagation constant β Is not known and needs to be found.

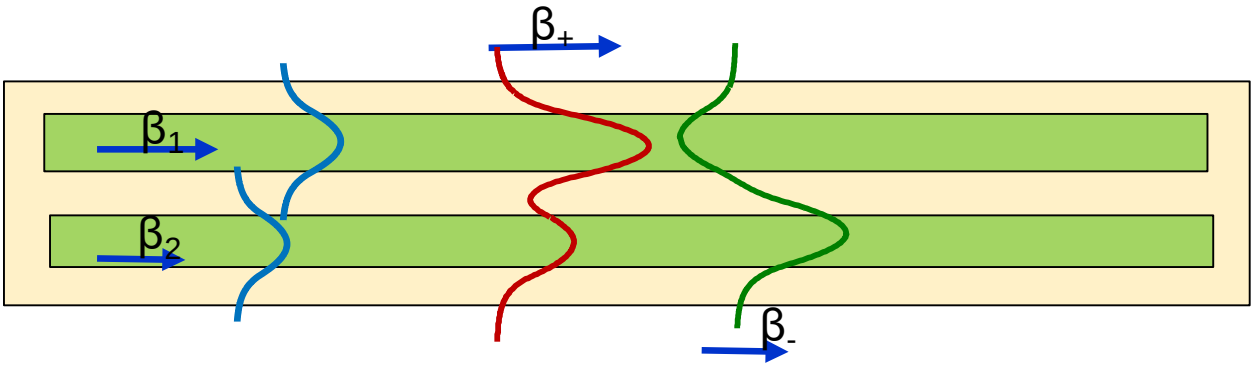

Figure 30.11. Supermodes concept – more general case

We know

If we substitute(30.83) into the Maxwell's equations (30.2) we obtain

$$\begin{aligned}\sum_{m=1}^{2} C_m\left(-\nabla_\perp \times \boldsymbol{e}_m + j\omega\mu \boldsymbol{h}_m\right)e^{j\beta z} &= \sum_{m=1}^{2} jC_m\beta\hat{\mathbf{z}}\times\boldsymbol{e}_m e^{j\beta z}\\ \sum_{m=1}^{2} C_m\left(-\nabla_\perp \times \boldsymbol{h}_m - j\omega\varepsilon_0 n^2(x,y)\boldsymbol{e}_m\right)e^{j\beta z} &= \sum_{m=1}^{2} jC_m\beta\hat{\mathbf{z}}\times\boldsymbol{h}_m e^{j\beta z}\end{aligned} \tag{30.84}$$

But we know that two modes 1 and 2 satisfy Maxwell's equations (30.21)

$$\begin{aligned}-\nabla_\perp \times \boldsymbol{e}_{1,2} + j\omega\mu \boldsymbol{h}_{1,2} &= j\beta_{1,2}\hat{\mathbf{z}}\times\boldsymbol{e}_{1,2}\\ -\nabla_\perp \times \boldsymbol{h}_{1,2} - j\omega\varepsilon_0 \overline{n}^2_{1,2}(x,y)\boldsymbol{h}_{1,2} &= j\beta_{1,2}\hat{\mathbf{z}}\times\boldsymbol{h}_{1,2}\end{aligned} \tag{30.85}$$

Therefore by substituting (30.85) into (30.84) we obtain

$$\begin{aligned}\sum_{m=1}^{2} C_m\beta_m\hat{\mathbf{z}}\times\boldsymbol{e}_m &= \sum_{m=1}^{2} C_m\beta\hat{\mathbf{z}}\times\boldsymbol{e}_m\\ \sum_{m=1}^{2} C_m\left[\beta_m\hat{\mathbf{z}}\times\boldsymbol{h}_m - \omega\varepsilon_0\delta n^2_{nm}(x,y)\boldsymbol{e}_m\right] &= \sum_{m=1}^{2} C_m\beta\hat{\mathbf{z}}\times\boldsymbol{h}_m\end{aligned} \tag{30.86}$$

Where we have used (30.20). We now combine all the terms on the l.h.s. and multiply the equations (30.86) by $\boldsymbol{h}_n^*$ and $\boldsymbol{e}_n^*$

$$\begin{aligned}\sum_{m=1}^{2} C_m\left(\beta_m-\beta\right)\left(\hat{\mathbf{z}}\times\boldsymbol{e}_m\right)\cdot\boldsymbol{h}_n^* &= 0\\ \sum_{m=1}^{2} C_m\left[\left(\beta_m-\beta\right)\left(\hat{\mathbf{z}}\times\boldsymbol{h}_m\right)\boldsymbol{e}_n^* - \omega\varepsilon_0\boldsymbol{e}_n^*\delta n^2_{nm}(x,y)\boldsymbol{e}_m\right] &= 0\end{aligned} \tag{30.87}$$

Subtracting the second line from the first one we obtain

$$\omega\varepsilon_0\sum_{m=1}^{2} C_m\left(\boldsymbol{e}_n^*\delta n_{nm}^2(x,y)\boldsymbol{e}_m\right)=\sum_{m=1}^{2}\left(\beta-\beta_m\right)\hat{\mathbf{z}}\cdot\left(\boldsymbol{e}_m\times\boldsymbol{h}_n^*+\boldsymbol{e}_n^*\times\boldsymbol{h}_m\right) \tag{30.88}$$

Now we integrate over the are *dxdy* and accommodate the diagonal terms $\iint \boldsymbol{e}_n^*\delta n_{nm}^2(x,y)\boldsymbol{e}_n dxdy$ and non-zero overlaps $\int\int\hat{\mathbf{z}}\cdot\left(\boldsymbol{e}_1\times\boldsymbol{h}_2^*+\boldsymbol{e}_2^*\times\boldsymbol{h}_1\right)dxdy$ as was done in (30.30)-(30.32) we obtain

$$\begin{aligned}\omega\varepsilon_0 C_2\int\int\boldsymbol{e}_1^*\delta n_{21}^2(x,y)\boldsymbol{e}_2 dxdy&=\left(\beta-\beta_1\right)C_1\int\int\hat{\mathbf{z}}\cdot\left(\boldsymbol{e}_1\times\boldsymbol{h}_1^*+\boldsymbol{e}_1^*\times\boldsymbol{h}_1\right)dxdy\\ \omega\varepsilon_0 C_1\int\int\boldsymbol{e}_2^*\delta n_{21}^2(x,y)\boldsymbol{e}_1 dxdy&=\left(\beta-\beta_2\right)C_2\int\int\hat{\mathbf{z}}\cdot\left(\boldsymbol{e}_2\times\boldsymbol{h}_2^*+\boldsymbol{e}_2^*\times\boldsymbol{h}_2\right)dxdy\end{aligned} \tag{30.89}$$

and

$$\begin{aligned}(\beta_1-\beta)C_1+\kappa C_2&=0\\ \kappa C_1+(\beta_2-\beta)C_2&=0\end{aligned} \tag{30.90}$$

where κ is the same as in (30.31). In matrix form

$$\begin{pmatrix}\beta_1-\beta & \kappa\\ \kappa & \beta_2-\beta\end{pmatrix}\begin{pmatrix}C_1\\ C_2\end{pmatrix}=0 \tag{30.91}$$

The equation, of course, has nontrivial solution only if determinant of matrix is zero and we obtain the characteristic equation

$$\beta^2-(\beta_1+\beta_2)+\beta_1\beta_2-\kappa^2=0 \tag{30.92}$$

leading us to two solutions:

$$\beta_{\pm}=\frac{\beta_1+\beta_2}{2}\pm\sqrt{\left(\frac{\beta_1-\beta_2}{2}\right)^2+\kappa^2}=\overline{\beta}+\sqrt{\Delta\beta^2+\kappa^2} \tag{30.93}$$

Where

$$\overline{\beta}=\frac{\beta_1+\beta_2}{2}\qquad\Delta\beta=\frac{\beta_1-\beta_2}{2} \tag{30.94}$$

Note that here we define $\Delta\beta$ as one half of the difference between propagation constants. We can re-write (30.90) as

$$\begin{aligned}(\overline{\beta}-\beta+\Delta\beta)C_1+\kappa C_2&=0\\ \kappa C_1+(\overline{\beta}-\beta-\Delta\beta)C_2&=0\end{aligned} \tag{30.95}$$

Now consider the first, larger propagation constant, solutions. If the mode is TE(TM)-like we can call it TE00 (TM00)

$$\beta_{00}=\beta_{+}=\overline{\beta}+\sqrt{\Delta\beta^2+\kappa^2} \tag{30.96}$$

Substitute it into (30.95) and obtain

$$C_2 = \frac{\sqrt{\kappa^2 + \Delta\beta^2} - \Delta\beta}{\kappa} C_1 \tag{30.97}$$

Here C_1 and C_2 have the same sign and $C_2 < C_1$. Since normalization requires $C_1^2 + C_2^2 = 1$ we obtain

$$\begin{aligned} C_1 &= \frac{1}{\sqrt{2}} \left(1 + \frac{\Delta\beta}{\sqrt{\kappa^2 + \Delta\beta^2}} \right)^{1/2} \\ C_2 &= \frac{1}{\sqrt{2}} \left(1 - \frac{\Delta\beta}{\sqrt{\kappa^2 + \Delta\beta^2}} \right)^{1/2}, \end{aligned} \tag{30.98}$$

The shape of the mode is shown in Fig.30.11.

The second, smaller propagation constant, solution is for the mode TE01 (TM01) and is

$$\beta_{01} = \beta_- = \overline{\beta} - \sqrt{\Delta\beta^2 + \kappa^2} \tag{30.99}$$

Substitution into (30.95) yields

$$\begin{aligned} C_1 &= -\frac{1}{\sqrt{2}} \left(1 - \frac{\Delta\beta}{\sqrt{\kappa^2 + \Delta\beta^2}} \right)^{1/2} \\ C_2 &= \frac{1}{\sqrt{2}} \left(1 + \frac{\Delta\beta}{\sqrt{\kappa^2 + \Delta\beta^2}} \right)^{1/2} \end{aligned} \tag{30.100}$$

Here C_1 and C_2 have the opposite signs and $|C_2| > |C_1|$. The mode has a node between two waveguides. If we introduce “asymmetry” parameter

$$f = \sqrt{\frac{\Delta\beta^2}{\kappa^2 + \Delta\beta^2}} \tag{30.101}$$

The modes can be written as

$$\begin{aligned} \boldsymbol{e}_+ &= \sqrt{\frac{1+f}{2}} \boldsymbol{e}_1 + \sqrt{\frac{1-f}{2}} \boldsymbol{e}_2 \\ \boldsymbol{e}_- &= -\sqrt{\frac{1-f}{2}} \boldsymbol{e}_1 + \sqrt{\frac{1+f}{2}} \boldsymbol{e}_2 \end{aligned} \tag{30.102}$$

Adiabatic coupling.

Note that when coupling is weak, i.e. $\kappa << \Delta\beta$ then $f \approx 1$ and

$$\begin{aligned} \boldsymbol{e}_+ &= \boldsymbol{e}_1 \\ \boldsymbol{e}_- &= \boldsymbol{e}_2 \end{aligned} \tag{30.103}$$

i.e. one has original, uncoupled modes. At the same time when coupling is very strong, $\kappa << \Delta\beta$, then $f \approx 0$, and

$$\boldsymbol{e}_\pm \approx \sqrt{\frac{1}{2}}\boldsymbol{e}_1 \pm \sqrt{\frac{1}{2}}\boldsymbol{e}_2 \tag{30.104}$$

i.e. pure symmetric and anti-symmetric modes. If the coupling is increased gradually (adiabatically), the two solutions do not mix, and the mode with larger propagation constant $\boldsymbol{e}_1$ gradually morphs into the symmetric mode $\boldsymbol{e}_+$ while $\boldsymbol{e}_2$ morphs into the anti-symmetric mode $\boldsymbol{e}_-$ as shown in Fig.30.12 It also works in reverse –one can separate symmetric and anti-symmetric modes.

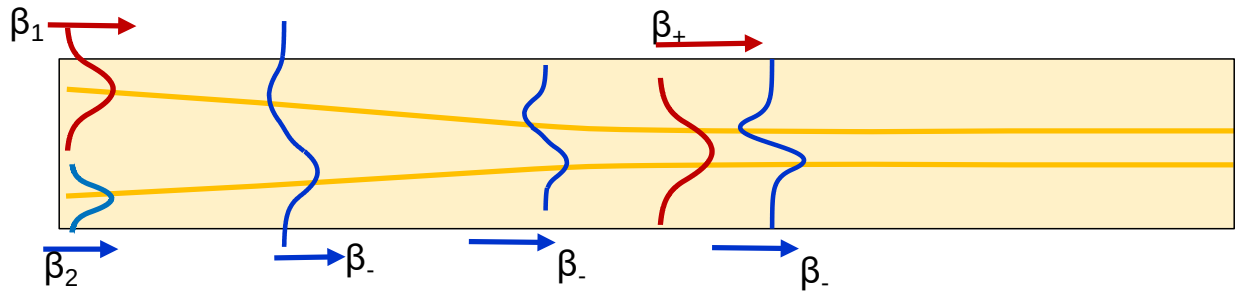

Figure 30.12 Adiabatic Y-coupler

Symmetric adiabatic 3dB Y-coupler

Consider the symmetric adiabatic coupler shown in Fig. 30.13.a..The light is entering from the waveguide 2 . One can write from (30.104)

$$\boldsymbol{e}_{1,2} = \sqrt{\frac{1}{2}}\boldsymbol{e}_+ \pm \sqrt{\frac{1}{2}}\boldsymbol{e}_- \tag{30.105}$$

Therefore, the input power evenly splits between symmetric (TE00) and antyi-symmetric (TE01) modes. As the waveguide narrows it becomes a single mode one – the anti-symmteric mod eis no longer propagating but radiating and at the output one only has symmetric mode. Thus only ½ of input power can be coupled into a single mode waveguide – a manifestation of conservation of spectral brightness. Obviously the same is true when the light enters at port 1 (Fig.30.13.b).

Situation is different though when one has equal powers entering from ports 1 and 2 and these outputs are in phase. Then one can write

$$A_{in}\boldsymbol{e}_1 + A_{in}\boldsymbol{e}_2 = A_{in}\left[\sqrt{\frac{1}{2}}\boldsymbol{e}_+ + \sqrt{\frac{1}{2}}\boldsymbol{e}_- + \sqrt{\frac{1}{2}}\boldsymbol{e}_+ - \sqrt{\frac{1}{2}}\boldsymbol{e}_-\right] = \sqrt{2}A_{in}\boldsymbol{e}_+ \tag{30.106}$$

Only symmetric mode gets excited so all the light gets coupled into the single mode waveguide and

$$P_{out} = 2P_{in} \tag{30.107}$$

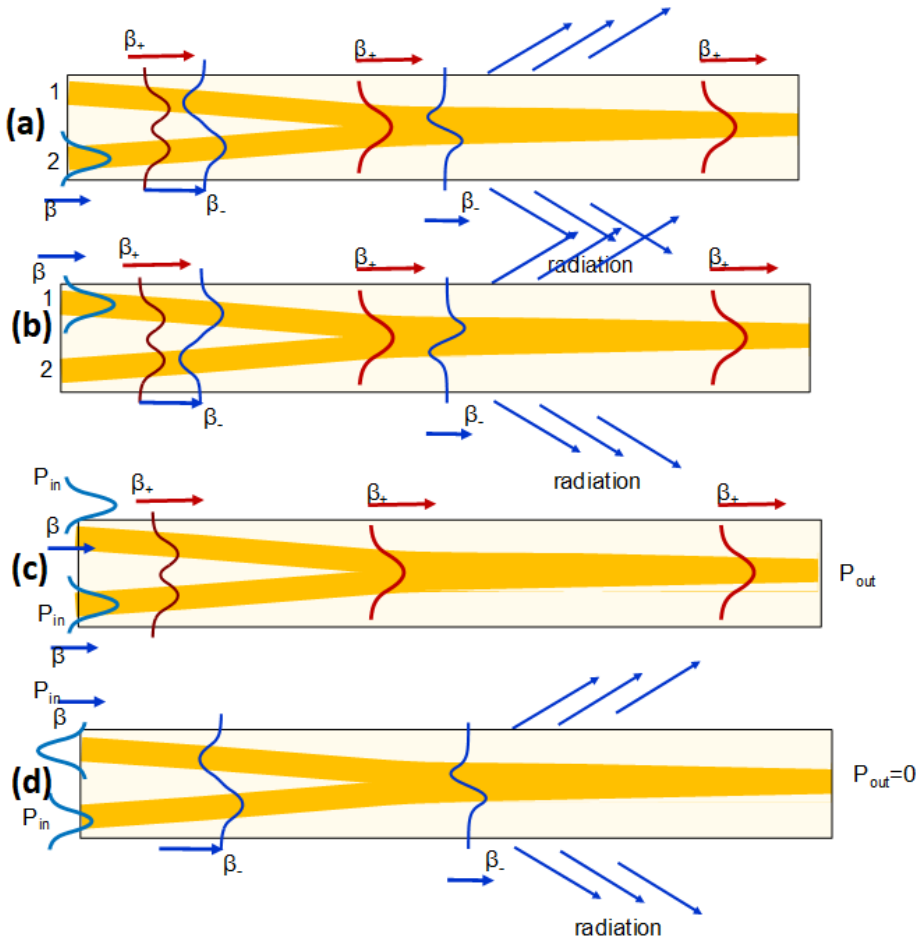

Figure 30.13. 3dB Y-coupler (a), (b) input in only one port (c) inputs are in phase (d) inputs are out of phase

If, on the other hand two equal inputs are 180 degrees out of phase as shown in Fig.30.13c , then

$$A_{in}\boldsymbol{e}_1 - A_{in}\boldsymbol{e}_2 = A_{in}\left[\sqrt{\frac{1}{2}}\boldsymbol{e}_+ + \sqrt{\frac{1}{2}}\boldsymbol{e}_- - \sqrt{\frac{1}{2}}\boldsymbol{e}_+ + \sqrt{\frac{1}{2}}\boldsymbol{e}_-\right] = \sqrt{2}A_{in}\boldsymbol{e}_- \tag{30.108}$$

Only the antisymmetric mode gets excited and as it propagates in the progressively narrowing waveguide it gets radiated. Thus $P_{out} = 0$. Y-couplers are used extensively in MZI modulators as one shown in Fig. 30.14 and that in addition to the electrodes to which AC modulated signal is applied to induce the phase shift (30.57) $\Delta\Phi_{12}(t) = \pi V(t)/V_\pi$ and contains an additional electrode to which DC bias is applied to provide bias phase shift $\Delta\Phi_0 = \pi V_{DC}/2V_\pi$

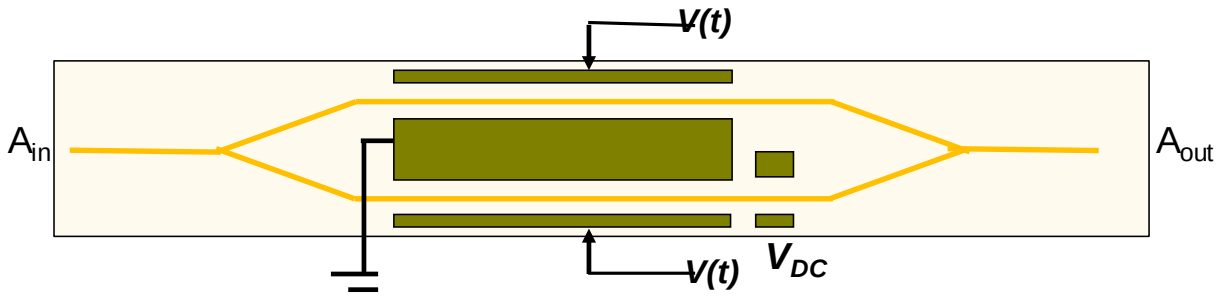

Figure 30.14 MZI modulator with Y couplers and DC bias

Therefore, the output is

$$A_{out} = A_{in}\cos(\Delta\Phi_{12}/2 + \Delta\Phi_0/2) \tag{30.109}$$

Consider first the case of MZI biased into null point,

$$V_{DC} = -V_\pi \quad \Phi_0 = -\pi/2 \tag{30.110}$$

So that the output is

$$\begin{aligned} A_{out}(t) &= A_{in}\sin(\pi V(t)/V_\pi) \\ P_{out}(t) &= P_{in}\sin^2(\pi V(t)/V_\pi) \end{aligned} \tag{30.111}$$

One can now use this configuration to achieve digital on-off keying (OOK) modulation as shown in Fig.30.15a. As voltage alternates between 0 and $V_\pi/2$ the output changes from 0 to P_{in} (multiplied by some insertion loss, of course).

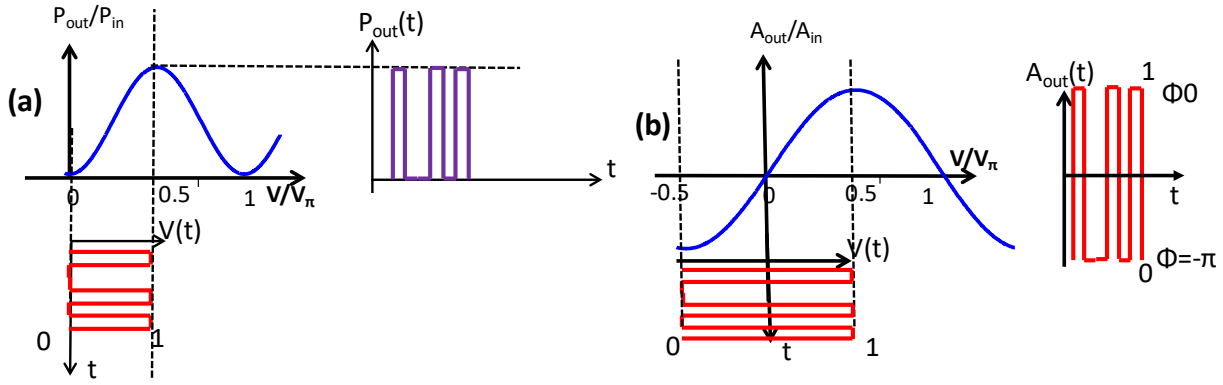

Figure 30.15 Digital modulation with MZI modulator (a) intensity modulation (b) amplitude modulation

One can also use this modulator to achieve binary phase shift configuration as shown in Fig.30.15b in which case the voltage swings between $-V_\pi/2$ and $+V_\pi/2$ so the phase of the output switches from π to 0.

Let us now turn to analog modulation. One may use the null-biased MZI modulator to achieve relatively linear amplitude modulation of signal – as shown in Fig.30.16a

$$A_{out}(t) = A_{in}\sin(\pi V(t)/V_\pi) \approx A_{in}\pi V(t)/V_\pi \tag{30.112}$$

– to detect this signal one must use local oscillator, as described above. If one uses direct detection in which photocurrent is proportional to the square of amplitude, the output won't be linear. To achieve (relatively) linear intensity analog modulation one uses MZI biased into quadrature, or

$$V_{DC} = -V_\pi/2 \quad \Phi_0 = -\pi/4 \tag{30.113}$$

The output power then is

$$\begin{aligned} P_{out}(t) &= P_{in}P_{in}\sin^2(\pi V(t)/V_\pi - \pi/4) = \frac{1+\cos(2\pi V(t)/V_\pi - \pi/2)}{2} = \\ &= \frac{P_{in}}{2} + \frac{P_{in}}{2}\sin\left(2\pi V(t)/V_\pi\right) \approx \frac{P_{in}}{2} + P_{in}\pi V(t)/V_\pi \end{aligned} \tag{30.114}$$

The AC component of photocurrent is roughly linear with V(t) as shown in Fig. 30.16b

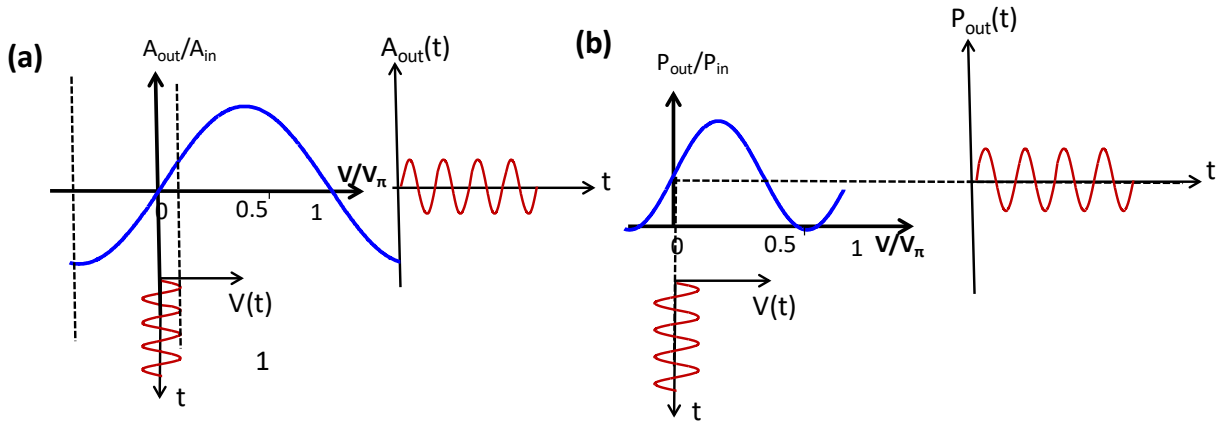

Figure 30.16 Analog modulation with MZI modulator (a) amplitude modulation (b) intensity modulation

Lithium niobate modulators

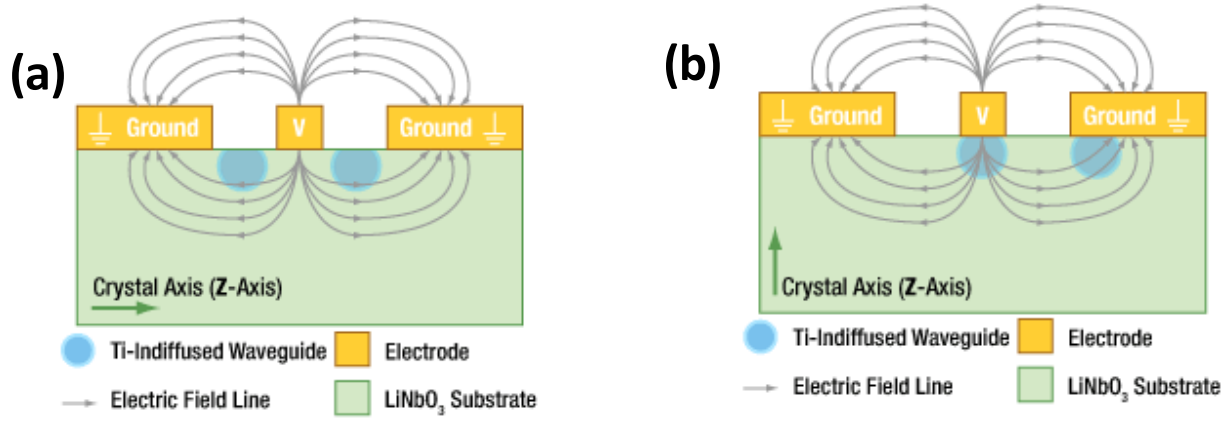

Figure 30.17 $LiNbO_3$ Intensity Modulator Cross-Section (a) X-cut (b) Z-cut.

Lithium niobate modulators use the largest Pockels coefficient $r_{33} = 30\,pm/V$. To use it both modulating field and optical wave must be directed along z-axis of the crystal (which happens to be optical axis) . This can be achieved by using either x-cut or z-cut crystal as shown in Fig.30.17 a and b respectively. In both cases one achieves push pull configuration. In bot cases the waveguide is diffused (some Nb atoms are substituted by Ta) and is wide – hence the effective width d_{eff} is rather large. Typical length is afew centimeters and V_π is few volts. Technical characteristics of $LiNbO_3$ are shown in Fig. 30.18

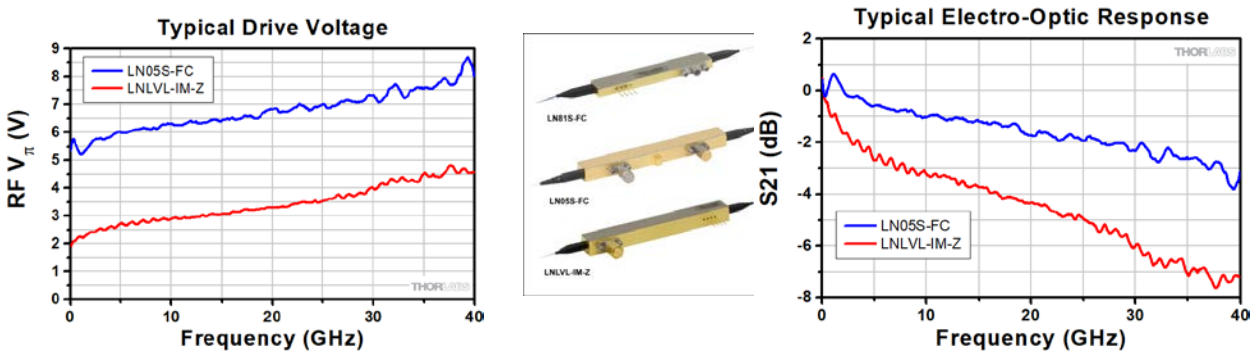

Figure 30.18 Typical Characteristics of lithium niobate modulators

Recently there have been exciting new developments – integration thin film $LiNbO_3$ on Si platform as shown in Fig.30.19 – the waveguides now are ridge waveguides and are much narrower than diffused ones. As a result half-wave voltage is only a couple of volts.

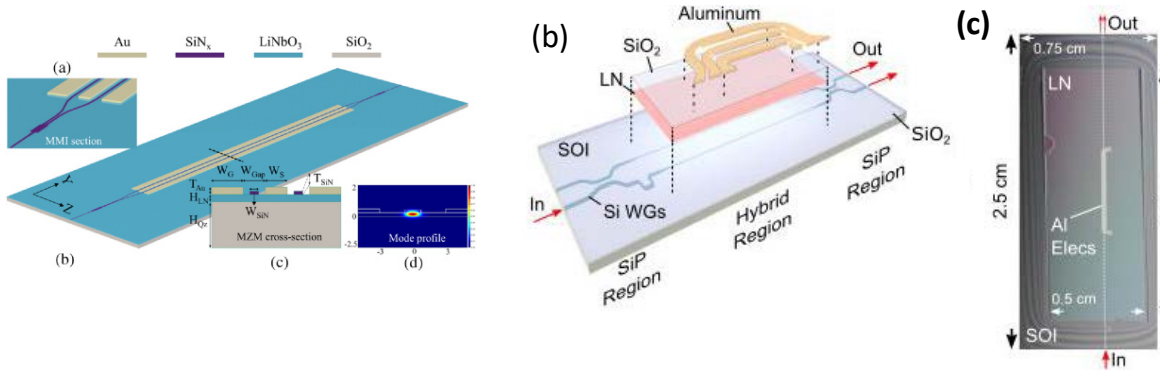

Figure 30.19 Thin Film $LiNbO_3$ on Si Modulators (a) SiN platform (b,c) SOI (silicon-on-isolator platform